A Method for Peak Power Prediction of Series-Connected Lithium-ion Battery Pack Using Extended Kalman Filter

Guangzhong Dong, Zonghai Chen, and Jingwen Wei
Department of Automation, University of Science and Technology of China (USTC), Hefei, China
Email: {dgz0725, chenzh, wei0519}@mail.ustc.edu.cn

***Abstract*—Rechargeable battery systems are key components of applications in on-board storage for Micro-grids and electric vehicles. One of the most important evaluation indexes for energy storage system is the peak power capability information, which is used to evaluate the instantaneous power capability of battery systems to release or absorb electrical energy. To give out an accurate peak power capability estimation method for series-connected lithium-ion battery pack, this paper first proposed an extended Kalman filter based state-of-charge estimation method. Then the estimated state-of-charges and predicted terminal voltages of the cells in a series-connected lithium-ion battery pack are regarded as the constraints of peak power capability. Finally, the proposed method is verified by experiments conducted on a 6-series LiFePO4 battery pack.**

***Index Terms*—battery storage, peak power capability, modeling, state estimation**

I. Introduction

The state-of-art Lithium-ion Batteries (LIBs) offer the best trade-off between energy/power density and costs for energy storage in electric vehicles and micro-grids [1], [2]. They are also featured by long life and environmental friendliness. Therefore, the LIB based energy storage systems have been finding applications in electric vehicles, smart grids and consumer electronics [3]. One of the most important evaluation indexes that the Battery Management System (BMS) must know is the peak power capability of batteries. Peak power capability information indicates the instantaneous power capability of battery systems to release or absorb electrical energy, which can be used to regulate the propelling power and to coordinate the regenerative braking and friction braking [4].

On the other hand, under-estimates of the peak power capability may result in overly conservative energy management, over-estimates of the peak power capability may cause the battery over-charge, over-discharge and premature failure [5]. However, the peak power capability is impossible to directly measure while the battery is working. The most commonly used method is the Hybrid Pulse Power Characterization (HPPC) method, which can only be employed in laboratory environments [5]. In the recent researches, the peak power capability is carried out with the design limits of the battery and powertrain. Such as [6] proposed a voltage – limited method for continuous peak power capability prediction to overcome the drawbacks of the HPPC method. Considering the state-of-energy (SOE) – limit or (state-of-charge) SOC – limit, and online parameter identification, which can only be employed in laboratory environments [7] and [8] proposed online model-based methods. The main concerned problem in these methods is how to carry out accurate SOC/SOE value.

In conclusion, to estimate peak power capability, an accurate battery model and an SOC/SOE estimation algorithm are necessary. However, as both the voltage and capacity of one single LIB are limited, hundreds/thousands cells must be connected in series and/or in parallel for high power applications [9]. Then, the estimation of peak power capability of battery pack is much more difficult than estimation of single cell's peak power, because the design limits of the battery and powertrain in a battery pack is much more complicated than that in one single cell.

To carry out estimation of peak power capability of battery pack, this paper first employs a first-order RC model to describe dynamics characteristics of series-connected battery pack. Then, extended Kalman filter method is used to estimate SOC of each cell [10], [11]. Finally, the peak power capability is carried out with the battery model, estimated SOC and the design limits of battery itself.

The outline of this paper is as following: the lumped parameter battery first-order RC model is given in Section II. The implement flowchart of the peak power capability estimator is given in Section III. The experiments, simulation results and evaluation of the proposed method are reported in Section IV. Finally, conclusions and final remarks are given in Section V.

II. Helpful Hints

Many types of battery models are used to evaluate the performances of batteries and to study their interactions with other electrical devices. Among them, the electric circuit models are much simpler for computation and analysis than electrochemical models [12], [13].

A widely used circuit based model for batteries is first-order RC model as depicted in Fig. 1 [14], [15].

Manuscript received July 13, 2016; revised January 2, 2017.

doi: 10.18178/ijmerr.6.2.134-139

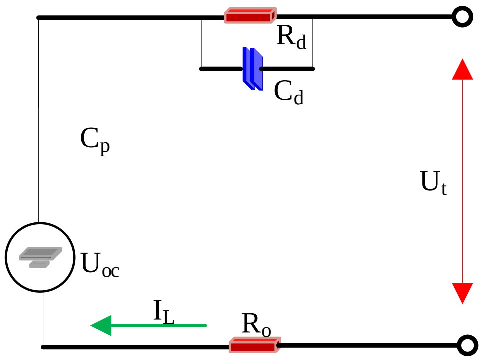

Figure 1. Note how the caption is centered in the column.

U_{oc} means ideal open circuit voltage. R_o is omhic resistor. C_d and R_d are polarized capacitor and resistor respectively. I_L is load current. U_t means the terminal voltage. The electrical behavior of the PNGV model can be expressed as (1).

$$\begin{aligned}&\begin{bmatrix} z_{k+1} \\ U_{d,k+1} \end{bmatrix} = \begin{bmatrix} 1 & 0 \\ 0 & \alpha \end{bmatrix}\begin{bmatrix} z_k \\ U_{d,k} \end{bmatrix} + \begin{bmatrix} -\Delta t/C_N \\ (1-\alpha)R_d \end{bmatrix} I_L \\ &U_{t,k} = U_{oc}(z_k) - R_o I_L - U_{d,k}\end{aligned} \tag{1}$$

where z is the abbreviation of SOC. U_d is the terminal voltage of the RC network. $\alpha_i = \exp(-\Delta t/R_i C_i)$. Δt is sampling time. C_N denotes the maximum available capacity of the battery.

III. Proposed Peak Power Capability Estimation Method

A. Extended Kalman Filter Based Soc Estimator

Extended Kalman filters have become a popular class of algorithms for solving the optimal estimation problems for non-linear state space models. A general formula for nonlinear dynamic system in (1) is shown in (2).

$$\begin{cases} \mathbf{x}_{k+1} = f(\mathbf{x}_k, \mathbf{u}_k) + \mathbf{w}_k \\ y_k = g(\mathbf{x}_k, \mathbf{u}_k) + v_k \end{cases} \tag{2}$$

where $\mathbf{x}_k$ is the state vector at discrete-time index k . $f(\cdot)$ and $g(\cdot)$ are state transition and measurement functions, respectively. The vector u_k is the measured exogenous system input at sampling k and $\mathbf{w}_k$ is the process noise with known pdfs: $\mathbf{w}_k \sim N(\mathbf{0}, \mathbf{\Sigma}_w)$ and is used to account for current-sensor error and inaccuracy of the state equation. y_k represents system output at discrete-time index k and $\mathbf{v}_k$ is the measurement noise with known pdfs: $v_k \sim N(0, \Sigma_v)$, which is used to account for voltage sensor error and inaccuracy of the output equation. The details of extended Kalman filter algorithm are summarized as follows [16]:

Step 1: Initialization:

For $k=0$, initial state and posteriori error covariance: $\hat{\mathbf{x}}_0^+ = E(\mathbf{x}_0)$, $\mathbf{P}_0^+ = E\left[\left(\mathbf{x}_0 - \hat{\mathbf{x}}_0^+\right)\left(\mathbf{x}_0 - \hat{\mathbf{x}}_0^+\right)^{\mathrm{T}}\right]$.

Step 2: Computation $k = 1, 2, \cdots$:

(a) Time update-prior estimation

Predicted state estimation:

$$\hat{\mathbf{x}}_k^- = f(\hat{\mathbf{x}}_{k-1}^+, u_{k-1}) + \mathbf{w}_{k-1} \tag{3}$$

Predicted estimation covariance

$$\mathbf{\Sigma}_{x,k}^- = \mathrm{A}_{k-1}\mathbf{\Sigma}_{x,k-1}^+\mathbf{A}_{k-1}^T + \mathbf{\Sigma}_w \tag{4}$$

(b) Measurement update:

Error innovation:

$$e_k = y_k - \hat{y}_k = y_k - g(\hat{\mathbf{x}}_k^-, u_k) \tag{5}$$

Innovation covariance:

$$S_k = \mathbf{C}_k^x \mathbf{\Sigma}_{x,k}^- (\mathbf{C}_k^x)^T + \Sigma_v \tag{6}$$

Optimal Kalman gain:

$$\mathbf{K}_k = \mathbf{\Sigma}_{x,k}^- (\mathbf{C}_k^x)^T S_k^{-1} \tag{7}$$

Updated state estimation:

$$\hat{\mathbf{x}}_k^+ = \hat{\mathbf{x}}_k^- + \mathbf{K}_k e_k \tag{8}$$

Updated estimation covariance:

$$\mathbf{\Sigma}_{x,k}^+ = (\mathbf{I} - \mathbf{K}_k \mathbf{C}_k^x)\mathbf{\Sigma}_{x,k}^- \tag{9}$$

The SOC of after completion of the algorithm is:

$$\hat{z}_k = \left[\hat{\mathbf{x}}_k^+\right]_1 \tag{10}$$

where $\mathbf{C}_k^x = \left.\frac{\partial g(\mathbf{x}_k, u_k, \hat{\mathbf{\theta}}_k^-)}{\partial \mathbf{x}_k}\right|_{\mathbf{x}=\hat{\mathbf{x}}_k^-}$, $\mathbf{A}_{k-1} = \left.\frac{\partial f(\mathbf{x}_{k-1}, u_{k-1}, \hat{\mathbf{\theta}}_k^-)}{\partial \mathbf{x}_{k-1}}\right|_{\mathbf{x}=\hat{\mathbf{x}}_{k-1}^+}$.

B. Estimation of Peak Power Capability

Herein, the load current of battery is assumed as positive for discharge and negative for charge. Then, to estimate peak power capability is related to predict maximum discharge current or minimum charge current. According to [3], the formulation of peak power capability of one single cell can be expressed as (11).

$$\begin{cases} P_{\min}^{\mathrm{chg}} = \max\left(P_{\min}, U_{t,k+L} I_{\min}^{\mathrm{chg}}\right) \\ P_{\max}^{\mathrm{dis}} = \min\left(P_{\max}, U_{t,k+L} I_{\max}^{\mathrm{dis}}\right) \end{cases} \tag{11}$$

where $P_{\min}^{\mathrm{chg}}(I_{\min}^{\mathrm{chg}})$ and $P_{\max}^{\mathrm{dis}}(I_{\max}^{\mathrm{dis}})$ denote the minimum charge power (current) and maximum discharge power (current) respectively. $P_{\min}$ and $P_{\max}$ are the power design limits of the battery. $U_{t,k+L}$ is the predicted terminal voltage at index $k+L$. Assumed that vehicular energy management require continuous power for acceleration, breaking or climbing conditions, during kth sampling time and $(k+L)$th sampling time, the input current of the battery can be assumed as a constant value. Considering a series-connected battery pack, (11) can be transformed as (12).

$$\begin{cases} P_{\min}^{\mathrm{chg}} = \max\left(P_{\min}, U_{t,k+L} \max\left(I_{\min,1}^{\mathrm{chg}}, I_{\min,2}^{\mathrm{chg}}, \cdots, I_{\min,N}^{\mathrm{chg}}\right)\right) \\ P_{\max}^{\mathrm{dis}} = \min\left(P_{\max}, U_{t,k+L} \min\left(I_{\max,1}^{\mathrm{dis}}, I_{\max,2}^{\mathrm{dis}}, \cdots, I_{\max,N}^{\mathrm{dis}}\right)\right) \end{cases} \tag{12}$$

To find the minimum continuous charging current $I_{\min}^{\text{chg}}$ and maximum continuous discharging current $I_{\max}^{\text{dis}}$ from kth sampling time to $(k+L)$th sampling time for ith cell, there are three constraints. N is the number of cells in a series-connected pack. *Terminal voltage constraint*:

$$U_{t,m} - \hat{U}_{t,k+L} = 0 \tag{13}$$

where $U_{t,m}$ is design limit of the upper cut-off voltage $U_{t,\max}$ for calculation of $I_{\min,i}^{\text{chg}}$, and is design limit of the lower cut-off voltage $U_{t,\min}$ for calculation of $I_{\max,i}^{\text{dis}}$. $\hat{U}_{t,k+L}$ is the prediction terminal voltage at index $k+L$. According to (13) and (1), the current capability of ith cell can be calculated by (14).

$$\begin{cases} I_{\max,i}^{dis,v} = \dfrac{U_{oc}(z_{k,i}) - U_{d,k,i}\alpha_i^L - U_{t,\min}}{\frac{L\Delta t}{C_{N,i}} \frac{\partial U_{oc}}{\partial z}\Big|_{z_{k,i}} + R_{d,i}(1-\alpha_i)\sum_{j=0}^{L-1}\alpha_i^{L-1-j} + R_{o,i}} \\ I_{\min,i}^{chg,v} = \dfrac{U_{oc}(z_{k,i}) - U_{d,k,i}\alpha_i^L - U_{t,\max}}{\frac{L\Delta t}{C_{N,i}} \frac{\partial U_{oc}}{\partial z}\Big|_{z_{k,i}} + R_{d,i}(1-\alpha_i)\sum_{j=0}^{L-1}\alpha_i^{L-1-j} + R_{o,i}} \end{cases} \tag{14}$$

1) *SOC constraint*

$$SOC_{t,m} - \hat{z}_{t,k+L} = 0 \tag{15}$$

where $SOC_{t,m}$ is design limit of the upper cut-off SOC $z_{\max}$ for calculation of $I_{\min}^{\text{chg}}$, and is design limit of the lower cut-off SOC $z_{\min}$ for calculation of $I_{\max}^{\text{dis}}$. $\hat{z}_{t,k+L}$ is the prediction SOC at index $k+L$. Then, the current capability of ith cell can be calculated by (16).

$$\begin{cases} I_{\min,i}^{\text{chg,z}} = \frac{(z_{k,i} - z_{\max})C_{N,i}}{L\Delta t} \\ I_{\max,i}^{\text{dis,z}} = \frac{(z_{k,i} - z_{\min})C_{N,i}}{L\Delta t} \end{cases} \tag{16}$$

2) *Design limits constraint*

The maximum discharging current and minimum charging current can be denoted as $I_{\max}$ and $I_{\min}$, respectively.

Combine (14) to (16), continuous current capability estimates with all constraints are calculated as (17).

$$\begin{cases} I_{\min,i}^{\text{chg}} = \max\left(I_{\min}, I_{\min,i}^{\text{chg,z}}, I_{\min,i}^{\text{chg,}v}\right) \\ I_{\max,i}^{\text{dis}} = \min\left(I_{\max}, I_{\max,i}^{\text{dis,z}}, I_{\max,i}^{\text{dis,}v}\right) \end{cases} \tag{17}$$

IV. Experiments and Discussion

In order to verify the proposed method, experimental studies were conducted on a 6-series-connected battery pack. Firstly, the parameters of test batteries are given out. The extended Kalman filter based estimator is then verified under different operating currents and temperatures. Finally, the peak power capability is estimated using the proposed method.

A. Parameters of Test Batteries

The parameters of the test batteries mainly contain open circuit voltage, ohmic resistance, total capacity, polarized capacitor and resistor. The open circuit voltages of 6 cells are plotted in Fig. 2. It can be seen that the open circuit voltages of the 6 cells are almost same in a large SOC range. After the HPPC (Hybrid Pulse Power Characteristic) tests, the ohmic inner resistances are shown in Fig. 3. From Fig. 3, it can be seen that the internal resistances during discharging are greater than that during charging. The numeric results of 3# cell are listed in Table I.

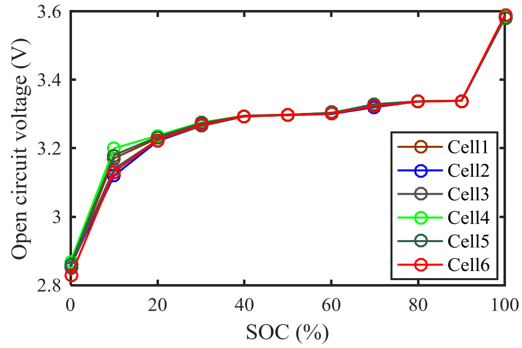

Figure 2. Open circuit voltage of six test cells.

TABLE I. Battery Parameters of 3# Cell.

SOC (%)	Parameters		
	OCV(V)	Resistance (mΩ)	
		Discharge	Charge
100%	3.583	-	-
90%	3.339	14.000	6.237
80%	3.337	14. 124	6.391
70%	3.322	14.206	6.495
60%	3.304	14.309	6.701
50%	3.297	14.495	6.856
40%	3.293	14.680	7.010
30%	3.265	14.804	7.216
20%	3.224	15.052	7.526
10%	3.14	15.650	8.041

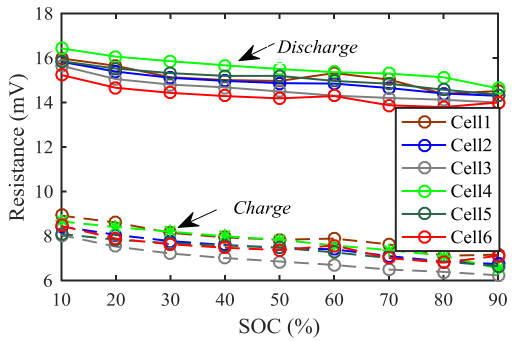

Figure 3. Inner resistance of six test cells.

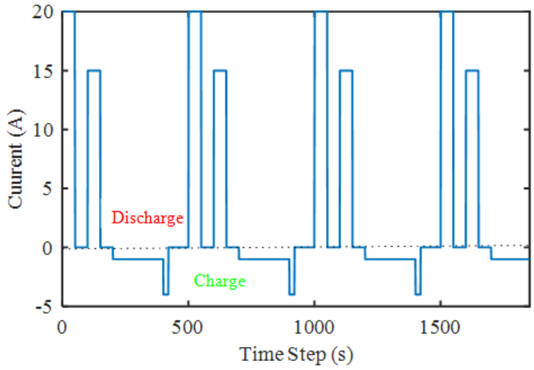

Figure 4. Dynamic current profile.

According to [15], The OCV function is expressed as follows:

$$U_{oc}(z) = K_0 + K_1 z + K_2/z + K_3 \ln(z) + K_4 \ln(1-z) \quad (17)$$

where z is the abbreviation of the SOC. K_i are five polynomial coefficients of the model. They are identified by apply the least squares method. The numerical results are show in Table II.

TABLE II. PARAMTERS OF THE OCV FUNCTION.

Parameters	Values (mV)
K_0	3526
K_1	–0.3744
K_2	315.9
K_3	151.6
K_4	–53.90

B. Verification of EKF Based Soc Estimator

Assumed the errors in modeling for parametric estimation are Δf_c and Δf_R, which represent capacity error and resistance error respectively. Thus, define:

$$\begin{cases} R_{o,\text{estimation}} = R_{o,\text{true}} + \Delta f_R \\ C_{N,\text{estimation}} = C_{N,\text{true}} + \Delta f_c \end{cases} \quad (19)$$

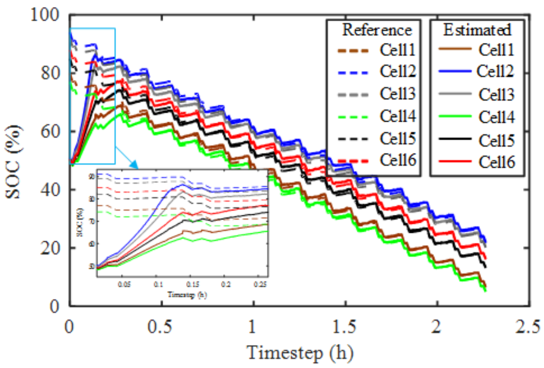

Figure 5. SOC estimation results.

In order to verify the EKF based SOC estimator. The test batteries are discharged with a dynamic current profile, as shown in Fig. 4. The six cells' SOC estimation results of the EKF method are plotted in Fig. 5, while the absolute errors are plotted in Fig. 6. The corresponding voltages are plotted in Fig. 7. The numeric results are listed in Table III. These results show that the proposed method provides high accuracy for estimating SOC under dynamic current conditions, even with an erroneous initial SOC.

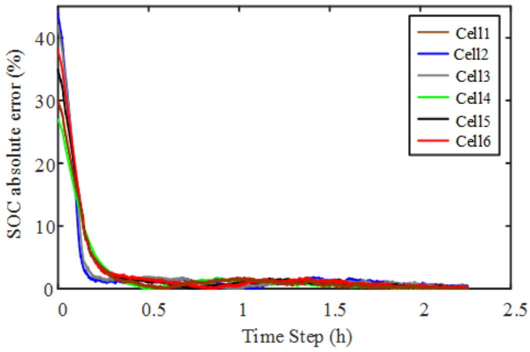

Figure 6. Absolute errors of SOC estimation.

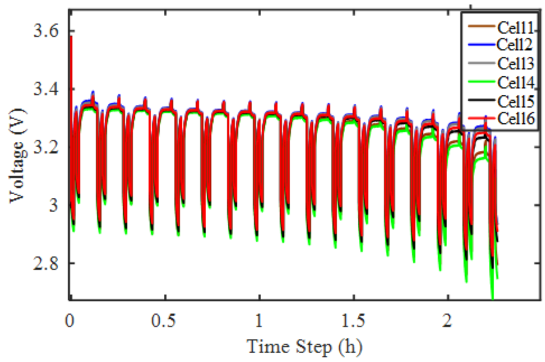

Figure 7. The six cells' terminal voltage.

TABLE III. NUMERICAL RESULTS OF SOC ESTIMATION.

Battery Number	RMSE[a]
1	5.48
2	6.86
3	6.80
4	5.08
5	6.21
6	6.62

a. RMSE = Root Mean Square Error.

C. Verfication and Discussion on Peak Power Prediction

Through the estimated battery SOC and predicted battery terminal voltage, the peak power capability can be calculated. Before the calculation for battery peak power, the design limits for battery current, power and SOC firstly, as shown in Table IV.

The maximum discharge current calculated from *Terminal voltage constraint* and *SOC constraint* are plotted in Fig. 8 and Fig. 9 respectively, while the minimum charge current from the two constraints are plotted in Fig. 10 and Fig. 11 respectively.

Firstly, it can be seen from Fig. 8-Fig. 11 that *Terminal voltage constraint-based* current capability is much smaller than *SOC constraint-based*. It is mainly because that SOC changes gently along with battery current. However, because of the existence of internal resistance, terminal voltage changes immediately once battery current changes.

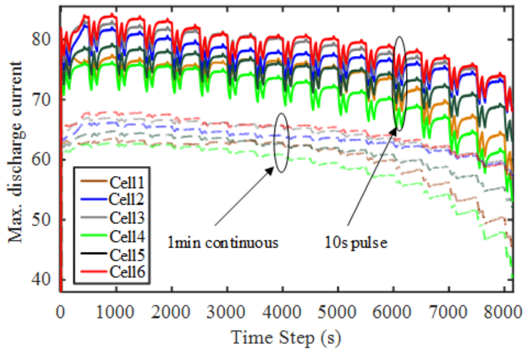

Figure 8. Max. discharge current from *Terminal voltage constraint*.

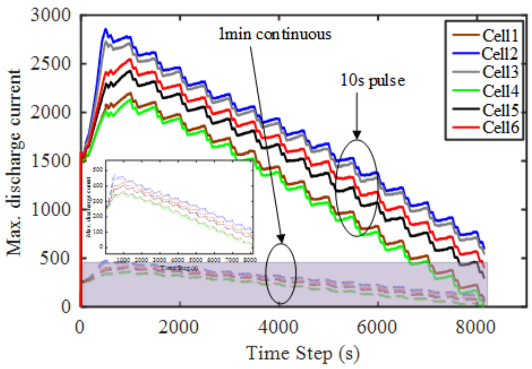

Figure 9. Max. discharge current *from SOC constraint*.

TABLE IV. DESIGN LIMITS FOR THE LIFEPO4 BATTERY CELL.

Current type	Power (W)	Current(A)	SOC(%)
Pulse(Dis/Chg)	130/-90	60/-40	5
Continuous(Dis/Chg)	50/-30	20/-10	95

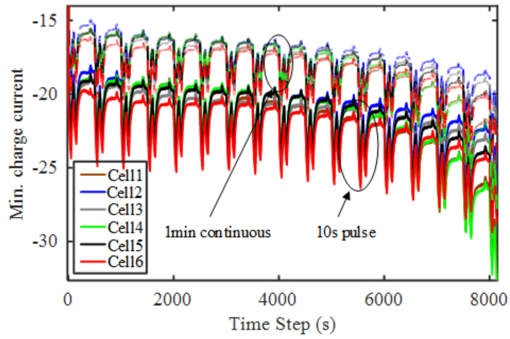

Figure 10. Min. charge current from *Terminal voltage constraint*.

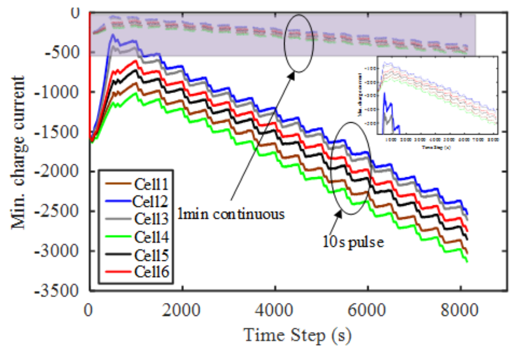

Figure 11. Min. *charge* current from *SOC constraint*.

Secondly, it can also be concluded that maximum discharge current of a battery pack is determined by the cell with minimum discharge current capability (4#), because of the buckets effect. Correspondingly, the minimum charge current of a battery pack is determined by the cell with maximum discharge current capability (2#).

Thirdly, it can also be concluded that there is a negative correlation between continuous current capability and sampling interval *L*. The current capability under 10s pulse current profiles are larger than 1min continuous current profiles.

Finally, the current capability calculated from bot *Terminal voltage constraint* and *SOC constraint* are much larger than battery design limits.

V. CONCLUSION

One of the most important evaluation indexes for energy storage system is the peak power capability which is used to evaluate the instantaneous power capability of battery systems to release or absorb electrical energy. Considering the series-connected lithium-ion battery pack, this paper provided a peak power prediction approach. Firstly, SOC information of in-pack cells is very important for battery peak capability prediction. Therefore, an EKF based method is employed to estimate SOC values of individual cells. Then, peak power of a battery pack is analyzed according to individual cells' design limits. Finally, verification and some discussions about the proposed method are given out. The experimental results show that the proposed method can accurately estimate battery SOC and peak power information.

ACKNOWLEDGMENT

This work was supported was supported by the National Natural Science Fund of China (Grant No. 61375079).

REFERENCES

[1] G. Dong, J. Wei, C. Zhang, and Z. Chen, "Online state of charge estimation and open circuit voltage hysteresis modeling of LiFePO4 battery using invariant imbedding method," *Applied Energy*, vol. 162, pp. 163-171, Jan. 2016.

[2] G. Dong, X. Zhang, C. Zhang, and Z. Chen, "A method for state of energy estimation of lithium-ion batteries based on neural network model," *Energy*, vol. 90, no. 1, pp. 879-888, July 2015.

[3] M. A. Roscger, O. S. Bohlen, and D. U. Sauer, "Reliable state estimation of multicell lithium-ion battery systems," *IEEE Trans. Energy Conversion*, vol. 26, no. 3, pp. 737-743, Sep. 2011.

[4] R. Xiong, F. Sun, H. He, and T. Nguyen, "A data-driven adaptive state of charge and power capability joint estimator of lithium-ion polymer battery used in electric vehicles," *Energy*, vol. 63, pp. 295-308, Dec. 2013.

[5] W. Zhang, W. Shi, and Z. Ma, "Adaptive unscented Kalman filter based state of energy and power capability estimation approach for lithium-ion battery," *Journal of Power Sources*, vol. 289, pp. 50-62, April 2015.

[6] G. L. Plett, "High-performance battery-pack power estimation using a dynamic cell model," *IEEE Trans. Veh. Technol.*, vol. 53, no. 5, pp. 1586-1593, Sep. 2004.

[7] R. Xiong, H, He, F. Sun, X. Liu, and Z. Zhen, "Model-based state of charge and peak power capability joint estimation of lithium-ion battery in plug-in hybrid electric vehicles," *Journal of Power Sources*, vol. 229, pp. 159-169, Dec. 2012.
[8] F. Sun, R. Xiong, and H. He, "Estimation of state-of-charge and state-of-power capability of lithium-ion battery considering varying health conditions," *Journal of Power Sources*, vol. 259, pp. 166-176, Feb. 2014.
[9] L. Zhang, C. Zhang, Y. He, and Z. Chen, "A method for the estimation of the battery pack state of charge based on in-pack cells uniformity analysis," *Applied Energy*, vol. 113, pp. 558-564, Aug. 2013.
[10] H. Dai, X. Wei, Z. Sun, J. Wang, and W. Gu, "Online cell SOC estimation of Li-ion battery packs using a dual time-scale Kalman filtering for EV applications," *Applied Energy*, vol. 95, pp. 227-237, Feb. 2012.
[11] F. Sun and R. Xiong, "A novel dual-scale cell state-of-charge estimation approach for series-connected battery pack used in electric vehicles," *Journal of Power Sources*, vol. 274, pp. 582-594, Oct. 2014.
[12] Y. He, X. Liu, C. Zhang, and Z. Chen, "A new model for State-of-Charge (SOC) estimation for high-power Li-ion batteries," *Applied Energy*, vol. 101, pp. 808-814, Aug. 2014.
[13] L. Devarakonda and T. Hu, "Algebraic method for parameter identification of circuit models for batteries under non-zero initial condition," *Journal of Power Sources*, vol. 268, pp. 928-940, June 2014.
[14] Y. Wang, C. Zhang, and Z. Chen, "An adaptive remaining energy prediction approach for lithium-ion batteries in electric vehicles," *Journal of Power Sources*, vol. 305, pp. 80-88, Feb. 2016.
[15] G. Dong, Z. Chen, J. Wei, Z. Chen, and P. Wang, "An online model-based method for state of energy estimation of lithium-ion batteries using dual filters," *Journal of Power Sources*, vol. 301, pp. 277-286, Jan. 2016.
[16] G. L. Plett, "Extended Kalman filtering for battery management systems of LiPB-based HEV battery packs: Part 1. Background," *Journal of Power Sources*, vol. 134, no. 2, pp. 252-261, August 12, 2004,

Guangzhong Dong was born in 1991. He received the B.E. degree in automation from University of Science and Technology of China, Hefei, China, in 2013, where he is currently working toward the Ph.D. degree in control Science and Engineering. His current research interests include the energy management for electric vehicle and smart micro-grids, the application of systems theory and optimization techniques to complex systems.

Zonghai Chen was born in 1963. He is currently a professor at the Laboratory of Simulation and Intelligent Control in the Department of Automation, University of Science and Technology (USTC). His research interests include simulation and optimization control of complex system, theory and technology of intelligent system, and quantum control theory.

Jingwen Wei was born in 1990. She received the B.E. degree in department of measurement-control technology and Instrument, from Heifei University of Technology, Heifei, China, in 2013. She is currently working toward the Ph.D. degree in control Science and Engineering with the University of Science and Technology of China, Hefei, China. Her current research interests include the energy management for electric vehicle and smart micro-grids, the application of systems theory and optimization techniques to complex systems.